The International Supercritical CO_2 Energy Technologies Symposium
March 2 - 5, 2026, Pittsburgh, PA
Paper #013

The Aerodynamic Design of a Multiphase-Tolerant Turbine for an sCO2 Heat Pump

Cole Replogle
Research Engineer
Southwest Research Institute
San Antonio, Texas

Dr. Natalie Smith
Manager, R&D
Southwest Research Institute
San Antonio, Texas

Dr. Evan Bond
Research Engineer
Southwest Research Institute
San Antonio, Texas

Mr. Cole Replogle is a Research Engineer in the Aero Thermal Modeling and Testing Sub-Section of the Machinery Department at Southwest Research Institute. He holds a B.S. in Aerospace Engineering and Mechanical Engineering from Oklahoma State University, and a Master of Research form the University of Cambridge. His interests include turbomachinery aerodynamics, heat transfer, geothermal energy, energy storage, industrial decarbonization, and advanced power cycles. His experience is primarily in the areas of CO2 turbomachinery, heat exchanger analysis, test loop design, and cycle modeling.

Dr. Natalie Smith is a Manager in the Aero Thermal Modeling and Testing Sub-Section of the Machinery Department at Southwest Research Institute. She holds a B.S. in Aerospace Engineering from California Polytechnic State University and both an M.S. and Ph.D. in Aeronautics and Astronautics from Purdue University. Her research interests include turbomachinery aerodynamics and aeromechanics, advanced instrumentation applications, and thermodynamic analysis for advanced energy systems. Her experience is in the areas of aerodynamic design and test, instrumentation, digital signal processing (particularly for turbomachinery applications), and cycle analysis for advanced power cycle and long duration energy storage (LDES) applications.

Dr. Evan Bond is a Research Engineer in the Aero Thermal Modeling and Testing Sub-Section of the Machinery Department at Southwest Research Institute. He holds a B.S. in Aerospace Engineering from Embry-Riddle Aeronautical University, an M.S. in Aeronautics and Astronautics and a Ph.D. in Mechanical Engineering both from Purdue University. His professional experience includes the aerodynamic design of turbomachinery, CFD simulations of high-speed turbomachines and complex fluid systems, test article and instrumentation development, and aerodynamic performance testing.

ABSTRACT

As the energy market continues to evolve with increased renewables, such as solar and wind energy, the need to balance energy demand with its availability has become increasingly more challenging. Long-duration energy storage technologies, such as pumped thermal energy storage (PTES), are potential solutions to this challenge with high potential round-trip efficiency (RTE), no

geological or geographical constraints, and low safety risks.

The charge mode of a PTES system operates a heat pump cycle, converting input power to thermal energy in hot and cold reservoirs. The low-pressure side of the cycle for a supercritical CO2 (sCO2) PTES operates just above the vapor-dome and potentially drives the turbine to expand into the dome, resulting in multiphase operation in the rear stages of the turbine.

This paper presents the design of a multiphase-tolerant CO2 turbine for the heat pump of a PTES system. Meanline analysis and 3D CFD is used to iterate a baseline design to have higher efficiency under multiphase conditions. Multiple challenges with multiphase CFD are discussed including whether or not to treat the fluid as a homogenous mixture, the treatment of vapor across a mixing plane, and real gas property table generation. The turbine design presented is still being iterated on but shows that isentropic efficiencies in excess of 85% are achievable with multiphase flow.

INTRODUCTION

The increasing penetration of renewable energy in the electrical grid continues to elevate the need for long-duration energy storage (LDES) technologies. Among the concepts under development, pumped thermal energy storage (PTES) systems using supercritical carbon dioxide (sCO_2) offer the potential for high round-trip efficiencies and compact system footprints [1,2]. In proposed sCO_2 PTES architectures, the turbine operates in charge mode by expanding CO_2 to a cold liquid state near, or directly into, the saturation dome. This has been shown to increase cycle coefficient of performance (COP) from 10 to 30% versus use of an expansion valve [3, 4].

Cycle analysis indicates that allowing the turbine expansion process to enter the vapor dome can increase overall system performance. However, the degree to which these benefits are realized depends strongly on the loss of turbine efficiency associated with vapor formation during expansion. Little is known about the aerodynamic or mechanical consequences of operating an sCO_2 turbine in a partially flashing regime. As a result, the performance penalties and design requirements for a turbine exposed to multiphase CO_2 remain uncertain.

This study addresses these gaps by examining the aerodynamic design process for modifying a baseline liquid-phase turbine to tolerate multiphase operation. The baseline geometry is a multistage pump-as-turbine where vapor forms only in the final stage. As such, the scope of the project was to modify the final stage to produce acceptable aerodynamic performance (nominally 80% isentropic efficiency). A combination of meanline analysis and CFD is used to assess performance impacts when expanding into the dome. The results provide a foundation for future development of multiphase-capable turbomachinery for PTES applications.

ANALYTICAL METHODS

The baseline turbine consists of seven stages, but only the final stage is exposed to conditions in which vapor formation occurs. The objective of this project is to design and ultimately test a quarter-scale prototype representing the final two stages of the machine. The design of the multiphase test loop is detailed in a previous publication [5]. All geometry creation and modification were performed using the AxSTREAM software suite. Blade profiles for the baseline configuration were extracted directly from the provided solid models using the AxSLICE tool. Only the guide vane and rotor of the final stage were modified for multiphase operation, while the upstream stage geometry was fixed.

A meanline analysis within AxSTREAM was used to iterate the redesigned geometry. Figure 1 shows the meanline analysis domain, with flow moving from left to right. Real-gas property tables for CO_2 were employed, and the meanline solver treats any two-phase points as a homogeneous mixture. For the final stage, the boundary conditions consisted of prescribed inlet flow angle to the stator, total pressure and temperature at the inlet, and a specified static pressure at the exit; the program then solves for mass flow. The primary design variables were the stator exit angle, which sets the throat area, and the rotor metal angles, which were iterated to achieve the target pressure ratio and mass flow while maintaining nominal incidence and exit swirl. As shown in Table 1, the resulting meanline predictions, particularly for mass flow and efficiency, show good agreement with the subsequent CFD analysis.

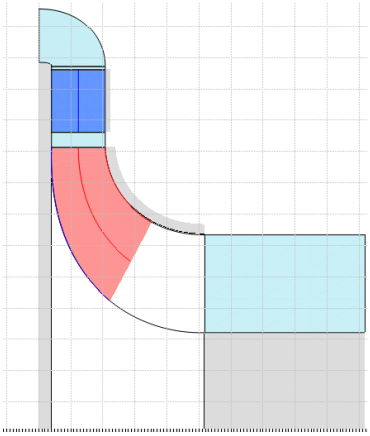

Figure 1. Meridional view of AxSTREAM meanline analysis domain.

Table 1. Comparison of meanline and CFD results for multiphase rotor stage.

	Meanline	**3D CFD**	**Unit**
Mass flow	336	369	**kg/s**
Rotor inlet relative flow angle	24	-2	**deg**
Rotor exit swirl angle	71	44	**deg**
Isentropic efficiency	86.9	87.3	**%**

ANSYS CFX was used to perform all 3D steady RANS simulations. Simulations employed the SST turbulence model with smooth, adiabatic walls. Meshing was performed in ANSYS Turbogrid, with input geometry from AxSTREAM. A grid-convergence study was conducted resulting in a final mesh of approximately 6 million elements. The final stage rotor has a finer mesh than the other domains, containing 2.75 million elements alone. The multistage rotor domain has a maximum y+ value of 25. The domains and interfaces are shown in Figure 2. Nomenclature from steam turbines has been adopted, where stage counts are often numbered from back-to-front. L0 is the final, multiphase stage and L1 is the upstream single phase stage. Boundary conditions consisted of inlet total pressure, total temperature, and a prescribed inlet vapor mass fraction of zero, with static pressure specified at the exit.

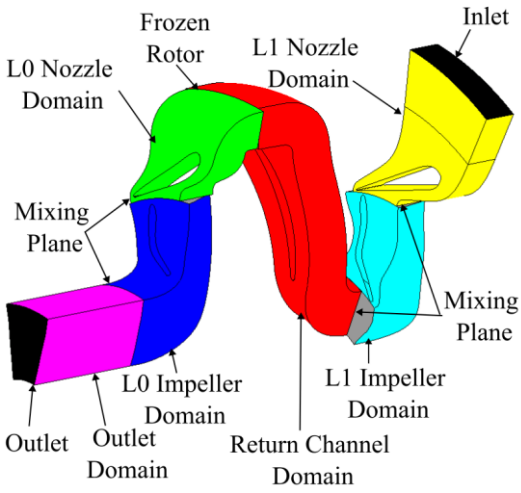

Figure 2. Two stage multiphase CO2 turbine fluid domains and interfaces

Real-gas-property (RGP) tables were used for the CO_2 fluid properties. These tables are generated by specifying the required pressure and temperature ranges along with a target interpolation error. Both the interpolation tolerance and the generation method significantly influence stability and solution quality. Although CFX includes a built-in RGP table generator, a script-based version is available that provides greater transparency and control over the table creation process. It is critical to verify that no failed points are present in the generated table, as these will invariably lead to solver crashes. Table generation behavior varies across CFX versions; for example, Version 20.1 uses REFPROP v9, which is generally more stable, but produces property values that differ from those obtained with later versions. This study used CFX Version 24.2 and REFPROP v10.

For stability and memory efficiency, a narrow pressure–temperature range was selected that was sufficient to encompass the expected solution domain, rather than generating a universally applicable table. This minimizes RGP file size and reduces memory demand at runtime. CFX defaults to clipping values to the maximum extent of the table, so it is recommended to explicitly specify the clipping behavior via CCL; clipping is common as the solver begins iterating. It is recommended to perform an RGP table size independence study similar to a mesh independence study. An interpolation error of 3×10^{-5} was used for all results presented here.

The working fluid was modeled as a homogeneous binary mixture, which is a critical assumption. Homogeneous modeling is often justified for sCO_2 compressors operating near the critical point due to the small density ratio between phases [6-10]. As illustrated in Figure 3, the density ratio for a multiphase compressor near the critical region may be as low as 2. In contrast, the turbine discharge conditions in this study correspond to a density ratio of approximately 9. For comparison, flashing LNG expanders may experience density ratios of order 117, which produce large radial pressure gradients in rotating machinery and drive phase separation, resulting in aerodynamic performance degradation and mechanical concerns [11]. This is why axial designs are typically preferred for flashing LNG applications. In theory, there exists a density-ratio threshold beyond which the flow can no longer be reasonably considered homogeneous, but it is not clear what this value is.

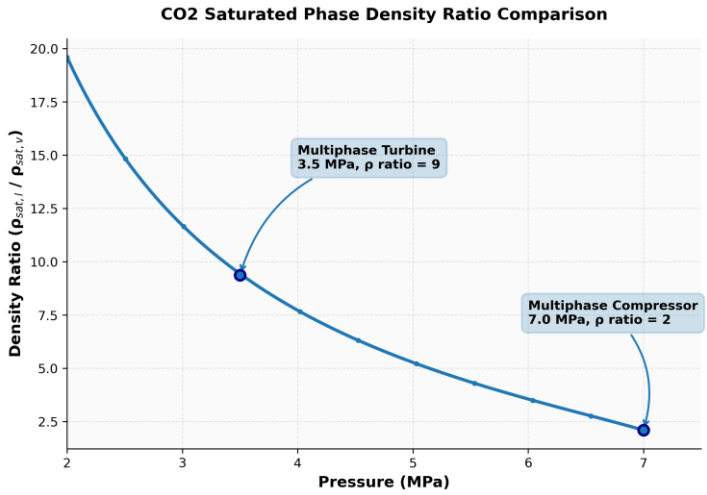

Figure 3. CO2 liquid-to-vapor density ratio as a function of pressure

Results from a companion nozzle test performed as part of this project suggest that a homogeneous assumption may underpredict losses for flashing CO_2 [12]. Nevertheless, the homogeneous mixture approach was adopted here for initial design evaluation, with planned follow-on work to assess alternative multiphase modeling strategies.

RESULTS AND DISCUSSION

Initial CFD analysis of the baseline geometry resulted in 118% of the target mass flow at the design pressure ratio, resulting in roughly 40 degrees of negative incidence on the rotor. To improve this, the guide vane and rotor trailing edge (TE) metal angles were iterated to achieve nominal incidence at the design mass flow and pressure ratio. In addition, the rotor hub and tip radii were increased to enlarge the flow passage area. Because the fluid density decreases substantially once vapor forms, this increase in area helps limit the corresponding rise in velocity and associated entropy generation.

The rotor chord and the vaneless space between the guide-vane TE and rotor leading edge (LE) were also increased. Changes to the rotor chord length had minimal aerodynamic impact. The vaneless space, however, had a significant influence on the predicted performance. Under the present boundary conditions, a “vapor front” forms near the rotor leading edge and extends upstream into the mixing plane interface between the stator and rotor. Increasing the vaneless space improved performance, though this effect may reflect limitations of steady RANS with a mixing-plane interface rather than a physical trend. A numerical approach without a mixing plane such as URANS should be performed to assess this with higher fidelity.

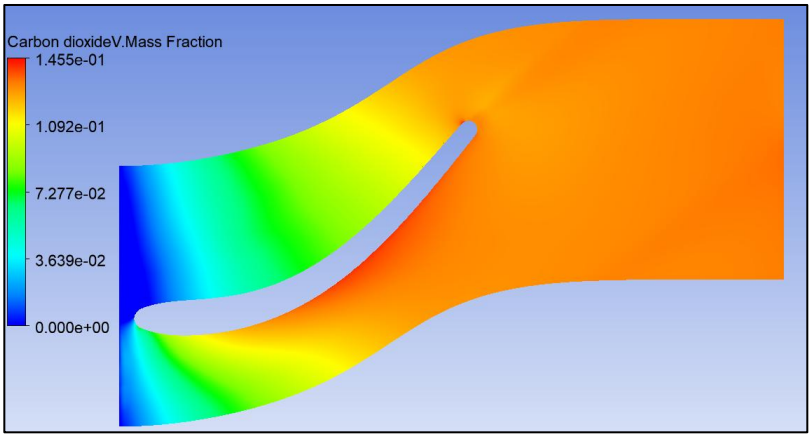

Figure 4. Contours of vapor mass fraction at midspan of multiphase rotor, showing interaction of vapor front with upstream mixing plane

A final geometry iteration was performed to address mechanical design considerations. The rotor chord was reduced and the hub radius increased, leading to a decrease in mass flow at the design pressure ratio and less ideal velocity triangles. Further iteration was not possible due to project time constraints. Table 2Table 3 summarizes the rotor inlet and exit conditions for the cases investigated. The resulting design exhibits higher incidence and increased exit swirl, as summarized in Table 3, but still attains an efficiency above the nominal 80% target.

Table 2. Multiphase rotor inlet and outlet fluid conditions

	Inlet	Outlet	Units
Density	833.0	440.0	[kg m^-3]
Vapor Mass Fraction	0.0046	0.1345	
Static Pressure	4823450	3465900	[Pa]
Total Pressure	6954830	3710800	[Pa]
Static Temperature	286.32	274.01	[K]
Total Temperature	289.09	276.77	[K]
Entropy	1118.58	1119.03	[J kg^-1 K^-1]
Relative Mach No.	0.03	0.21	

Table 3. Multiphase stage (guide vane and rotor) performance

Isentropic Efficiency (Last Stage GV and Rotor)	87.29	[%]
Mass flow / Target Mass Flow	99	[%]
Rotor Incidence	-5	[degree]
Rotor Exit Swirl	44	[degree]

As shown in Figure 5, increasing vapor formation leads to a substantial reduction in the local speed of sound, accompanied by a decrease in density. Despite these property changes, the Mach numbers in the present design remain very low. Special consideration would be required in cases where velocities approach sonic conditions, as the appropriate treatment of multiphase speed of sound is non-trivial. Figure 5 also highlights a pronounced flow-recirculation region on the pressure surface of the rotor. This feature appeared both in the baseline geometry, which operated with large negative incidence, and in the modified geometry, which exhibits relatively

high positive incidence.

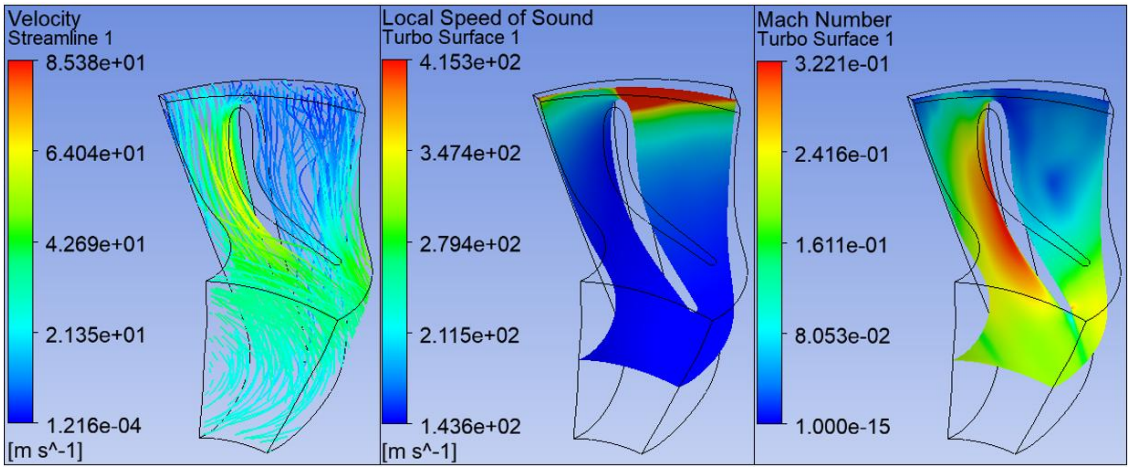

Figure 5. Multiphase rotor velocity streamlines (left), local speed of sound (center), and Mach Number (right)

Figure 6 presents the entropy generation through the machine, showing that the second-stage rotor experiences higher loss than the first-stage, single-phase rotor; however, most of the loss is generated near the stator trailing edge. This is attributed to the interaction of vapor formation with the mixing-plane interface, as discussed previously. The behavior was consistent across all mesh densities and boundary conditions examined. Increasing the distance between the guide-vane trailing edge and the rotor leading edge reduced the magnitude of this loss, though this is likely an artifact of the steady-state CFD approach rather than a physical trend.

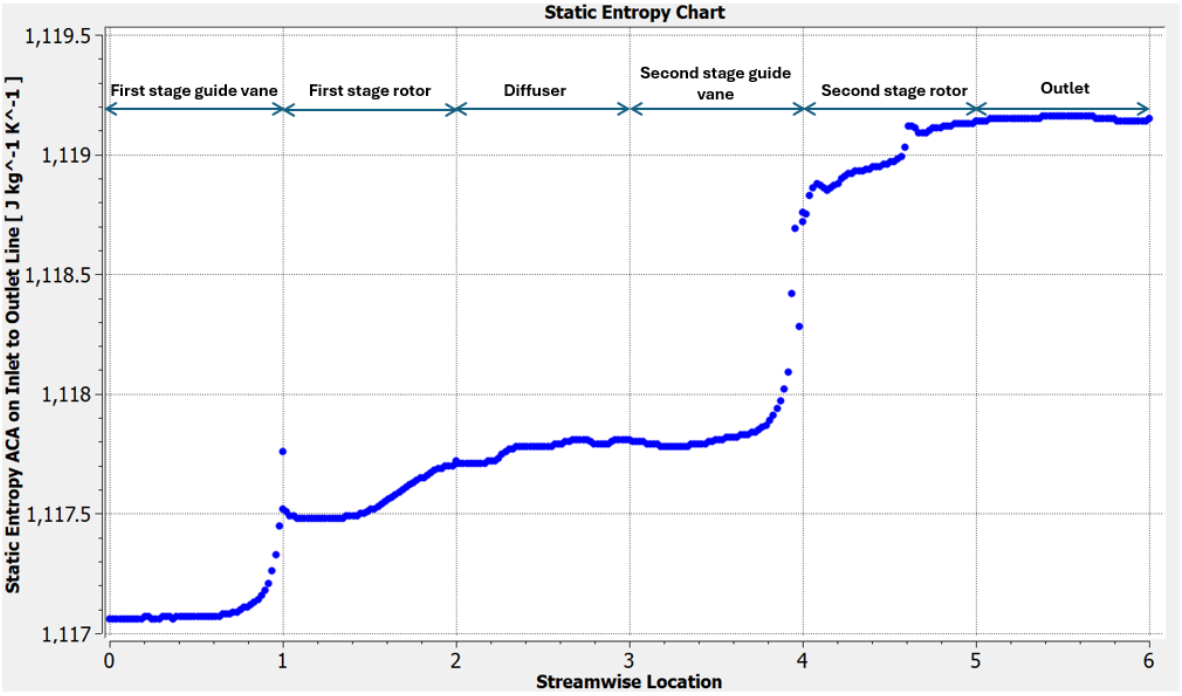

Figure 6. Streamwise development of entropy through machine

Figure 7 provides a meridional view of the multiphase rotor domain. The results indicate that

there is not a strong radial variation in vapor content, though this may also be a consequence of the homogeneous mixture assumption. No specific measures were taken to control radial gradients; however, if the real flow exhibits significant non-homogeneity, features such as blade sweep or lean may be required to minimize performance penalties. Additionally, the rotor blade profile, both thickness distribution and metal angles, was kept essentially unchanged from the baseline design. Should the flow prove to be non-homogeneous, more precise control of blade loading could be used to influence the onset location of vapor formation and improve overall performance.

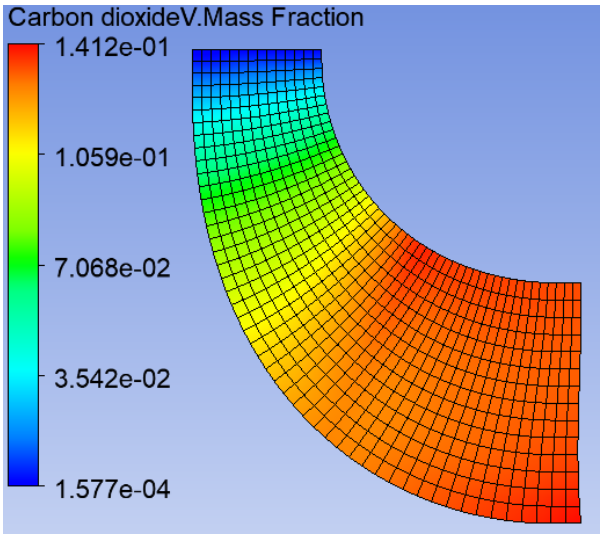

Figure 7. Meridional view of multiphase rotor fluid domain with contours of vapor mass fraction

CONCLUSIONS

This study presents a first-of-its-kind CFD investigation of a multiphase sCO_2 turbine. The results indicate that high efficiencies are achievable even when the expansion process enters the vapor dome. The velocity triangles differ substantially from those of a single-phase turbine, yet the machine maintains relatively low velocities throughout despite the density reduction associated with vapor formation. Additional design iteration could further refine the geometry to reduce incidence on the rotor. It is important to note, however, that turbine performance may differ significantly if the flow is not truly homogeneous and phase separation occurs. The presence of vapor at the mixing-plane interface may also influence the predicted losses. Future work will include evaluation of off-design operating conditions, transient simulations to better capture unsteady multiphase behavior, and testing of a quarter-scale prototype to validate the numerical findings.

REFERENCES

[1] Held, 2021, “Low-cost, long-duration electrical energy storage using a CO2 -based Electro Thermal Energy Storage (ETES) system” ARPA-E DAYS Annual Meeting, March 1-2, 2021.

[2] McTigue, Farres-Antunez, Ellingwood, Neises, White, 2020, “Pumped thermal electricity storage with supercritical CO2 cycles and solar heat input,” AIP Conference Proceedings 2303, 190024.

[3] Aghagoli, Sorin, Khennich, “Exergy Efficiency and COP Improvement of a CO2 Transcritical

Heat Pump System by Replacing an Expansion Valve with a Tesla Turbine," Energies. 2022, 15(14):4973.

[4] Murthy, Subiantoro, Norris, Fukuta, "A review on expanders and their performance in vapour compression refrigeration systems" International Journal of Refrigeration, 106 (2019)

[5] Smith, N. R., Replogle, C., Roddy, R., Brown, Z., McCandless, C., and Hofer, D., 2025, "Design of a Multiphase CO_2 Turbine Test Facility," Proceedings of ASME Turbo Expo 2025: Turbomachinery Technical Conference and Exposition, Memphis, TN, USA, June 16–20, Paper No. GT2025-154034.

[6] Hosangadi, Ashvin, et al. "Numerical Predictions of Mean Performance and Dynamic Behavior of a 10 MWe SCO2 Compressor With Test Data Validation." Journal of Engineering for Gas Turbines and Power 144.12 (2022): 121019.

[7] Hosangadi, Ashvin, et al. "Numerical Predictions of Mean Performance and Dynamic Behavior of a 10 MWe SCO2 Compressor With Test Data Validation." Journal of Engineering for Gas Turbines and Power 144.12 (2022): 121019.

[8] Persico, Giacomo, et al. "Implications of phase change on the aerodynamics of centrifugal compressors for supercritical carbon dioxide applications." Journal of Engineering for Gas Turbines and Power 143.4 (2021): 041007.

[9] Baltadjiev, Nikola D., Claudio Lettieri, and Zoltán S. Spakovszky. "An investigation of real gas effects in supercritical CO2 centrifugal compressors." Journal of Turbomachinery 137.9 (2015): 091003.

[10] Toni, Lorenzo, et al. "Computational and experimental assessment of a MW-scale supercritical CO2 compressor operating in multiple near-critical conditions." Journal of Engineering for Gas Turbines and Power 144.10 (2022): 101015.

[11] Kaupert, Kevin, et al. "Flashing liquid expanders for LNG liquefaction trains." Proceedings of 17th International Conference & Exhibition on Liquefied Natural Gas (LNG 17). Gas Technology Institute (GTI), Houston, USA. (2013).

[12] Replogle, C., Witt, K., Smith, N., Anguiano, M., and Koley, S. S., 2025, "Experimental Investigation of Vapor Formation in Liquid CO_2 Flow Through a Converging-Diverging Nozzle," Proceedings of ASME Turbo Expo 2025: Turbomachinery Technical Conference and Exposition, Memphis, TN, USA, June 16–20, Paper No. GT2025-154157.

DISCLAIMER

ACKNOWLEDGEMENTS

This material is based upon work supported by the U.S. Department of Energy's Office of Energy Efficiency and Renewable Energy (EERE) under the Solar Energy Technologies Office, Award Number DE-EE0009815.